Supporting Information

Selection Strategy of Porphyrins for Achieving Thermally Stable Polymer Solar Cells

Sisi Wang,[abc] Meiyan Wang,[§] Zhaobin Chen[ab], Xiaoniu Yang*[a]

[a]State Key Laboratory of Polymer Physics and Chemistry, Changchun Institute of Applied Chemistry, Chinese Academy of Sciences, 5625 Renmin Street, Changchun 130022, P. R. China..

[b]Polymer Composites Engineering Laboratory, Changchun Institute of Applied Chemistry, Chinese Academy of Sciences, 5625 Renmin Street, Changchun 130022, P. R. China.

[c]University of Chinese Academy of science, 19 Yuquan Road Shijingshan District, Beijing 100049, P.R. China.

[§] Institute of Theoretical Chemistry, Jilin University, Changchun 130023, P.R. China.

*E-mail: xnyang@ciac.ac.cn

Computational details

All the geometries were optimized without constraints by using the B97-D Grimme's functional,[1] which includes an additional dispersion energy term, and the 6-31G* basis set. The singlet state was calculated for all the porphyrins and porphyrin/C_{60} complexes corresponding to the ground state except for Cu-based ones for which the doublet state was considered. Frequency calculation was carried out at the same level of theory to identify all the geometries as minima (zero imaginary frequencies). On the B97-D/6-31G* optimized geometries, the single-point energy calculation was performed by using the PBE0 hybrid correlation-exchange functional,[2] which has been used in describing the weak intermolecular interactions,[3-4] in combination with the correlation-consistent cc-pVTZ basis set.[5] The Grimme's D3 dispersion correction with Becke-Johnson damping

function was applied.[6] The binding energy (E_b) of the porphyrin/C_{60} supramolecular complex was computed as the difference between the energy of porphyrin/C_{60} and the sum of the energies of porphyrin and C_{60}, i.e., E_b= E(porphyrin/C_{60}) – [E(porphyrin) + E(C_{60})]. All calculations were performed with the Gaussian 09 software package.[7]

Table S1 displays the 3D structural disposition adopted by the porphyrin- and the methanofullerene-based moieties in all the associates. Considering the difference of BL6/C_{60} and BL6 from the corresponding supramolecular complexes and free porphyrins, the triplet states of BL6/C_{60} and BL6 were calculated to compare with the above discussed singlet states of BL6/C_{60} and BL6. The triplet state of BL6/C_{60} has the similar structure as the other five supramolecular complexes with Ni locating above an electron-rich 6:6 double bond of C_{60}, and the porphyrin plane in triplet state of BL6 is also slightly distorted as free BL0-BL5 porphyrins. From calculations at the B97-D/6-31G* level of theory, the triplet states of BL6/C_{60} and BL6 are 4.0 and 20.4 kcal/mol, respectively, higher in electronic energy than the corresponding singlet states, indicating that the ground states of BL6/C_{60} and BL6 are singlet, consistent with the experimental observation that the BL6/C_{60} supramolecular complex is diamagnetic.

Table S1 Minimum-energy structures computed at the B97-D/6-31G* level of theory for the supramolecular associates.

Complex	Bottom-view	Side-view
BL0(2H)/C_{60}	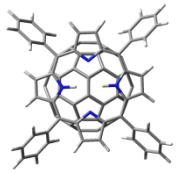	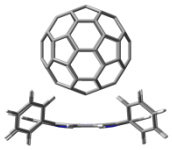
BL1(C_4F_7Cl)/C_{60}	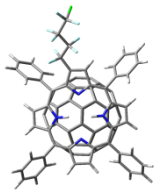	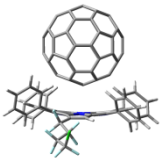
BL2(NO_2)/C_{60}	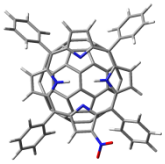	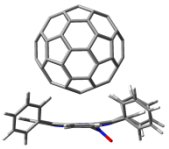
BL3(Cu&NO_2)/C_{60}	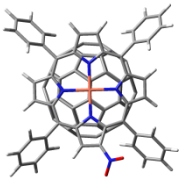	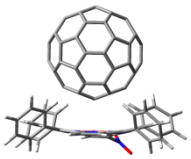
BL4(Cu)/C_{60}	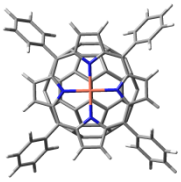	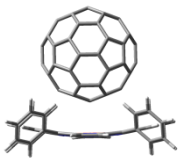
BL5(Zn)/C_{60}	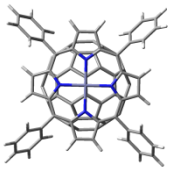	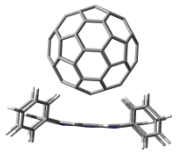
BL6(Ni)/C_{60}	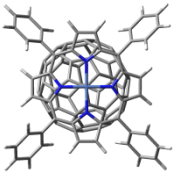	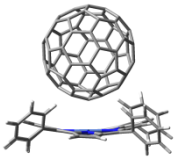

Table S2 The dihedral angles between the outer ring of single and double bonds.

Number / Porphyrin	1	2	3	4	5	6	7	8
BL0	5.129	6.264	6.275	5.135	5.141	6.268	6.264	5.134
BL1	8.957	6.639	7.974	5.903	7.139	11.993	19.286	4.256
BL2	6.690	7.328	8.022	8.353	6.371	17.103	11.11	5.73
BL3	9.390	8.547	8.931	10.436	8.109	17.372	11.372	8.013
BL4	7.425	5.518	7.441	5.526	7.439	5.512	7.43	5.511
BL5	4.414	4.565	4.468	4.576	4.543	4.633	4.519	4.551
BL6	3.164	13.899	3.164	13.904	3.163	13.909	3.157	13.906

Note: The dihedral angles $\angle N_1C_2C_3C_4$, $\angle C_2C_3C_4N_5$, $\angle N_5C_6C_7C_8$, $\angle C_6C_7C_8N_9$, $\angle N_9C_{10}C_{11}C_{12}$, $\angle C_{10}C_{11}C_{12}N_{13}$, $\angle N_{13}C_{14}C_{15}C_{16}$, $\angle C_{14}C_{15}C_{16}N_1$ are marked in sequence as 1, 2,……8.

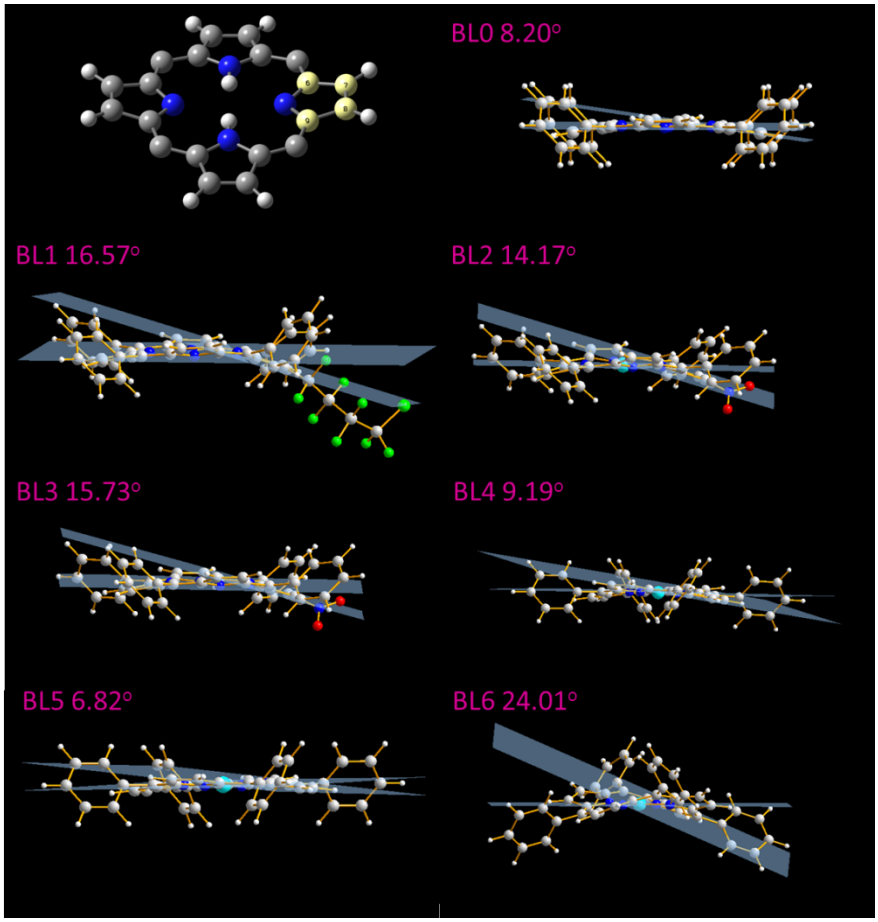

Fig. S1. The angles between the plane almost consisting of four N atoms and the plane of pyrrole ring calculated by Diamond software.

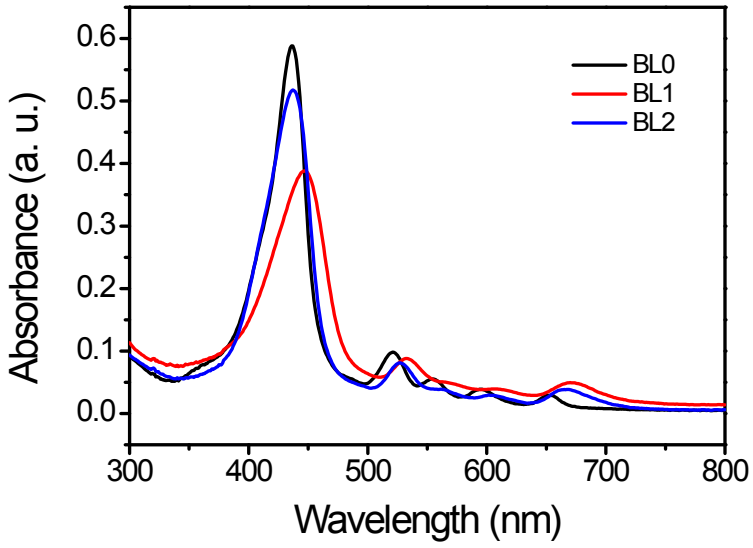

Fig. S2 UV-vis absorption spectra of BL0, BL1, and BL2 solutions in ODCB.

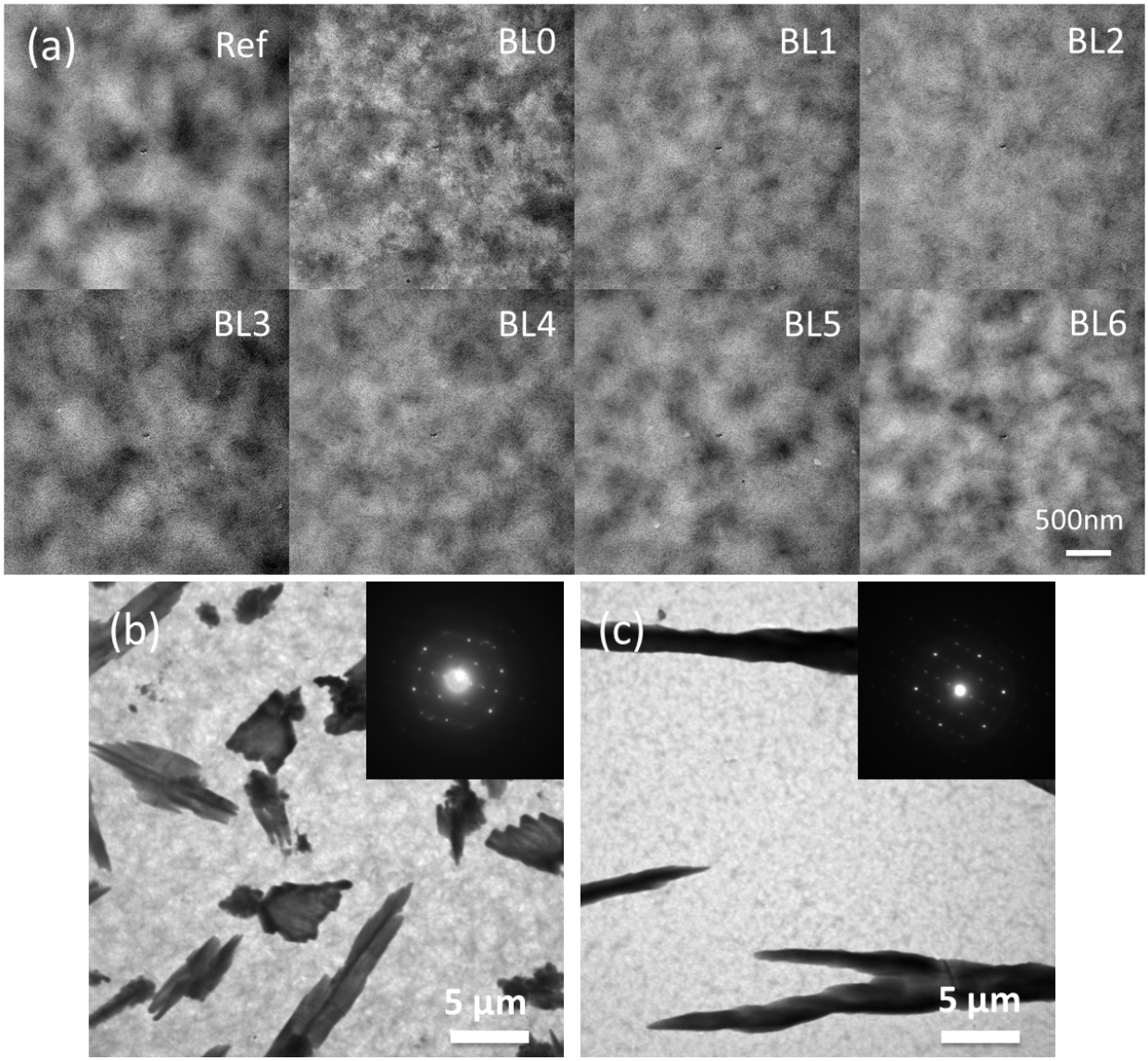

Fig. S3. TEM images of (a) pristine P3HT:$PC_{61}BM$:porphyrin (3.78%) blend films, (b) annealed P3HT:$PC_{61}BM$, and (c) annealed P3HT:$PC_{61}BM$:BL3 (3.78%) blend films at 130 ^{o}C for 1 and 12 h, respectively. Inserts are the SAED patterns of corresponding aggregates.

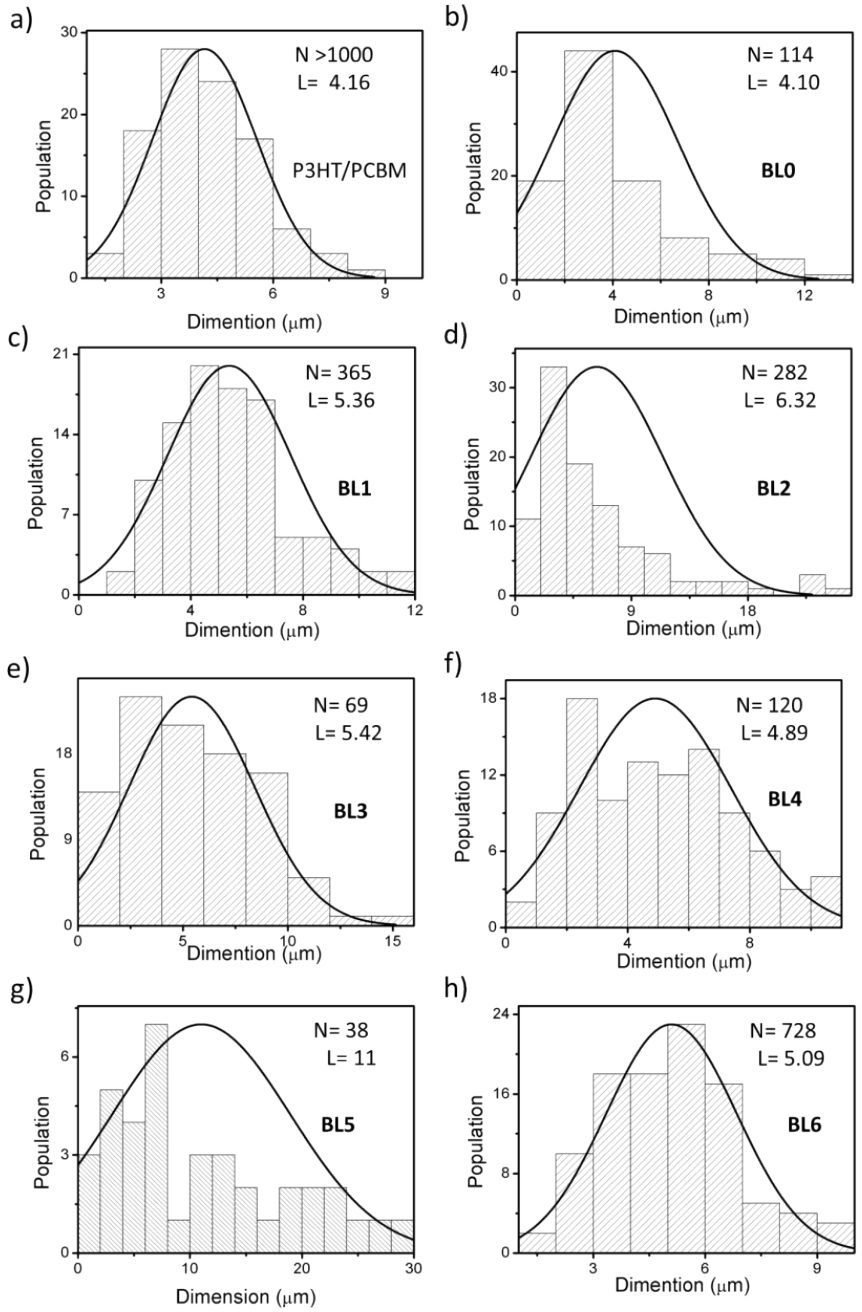

Fig. S4. Statistical histogram of the number and size of $PC_{61}BM$ aggregates in OM images shown in Figure 3. N is the total number and L (μm) is the average length of the $PC_{61}BM$ aggregates.

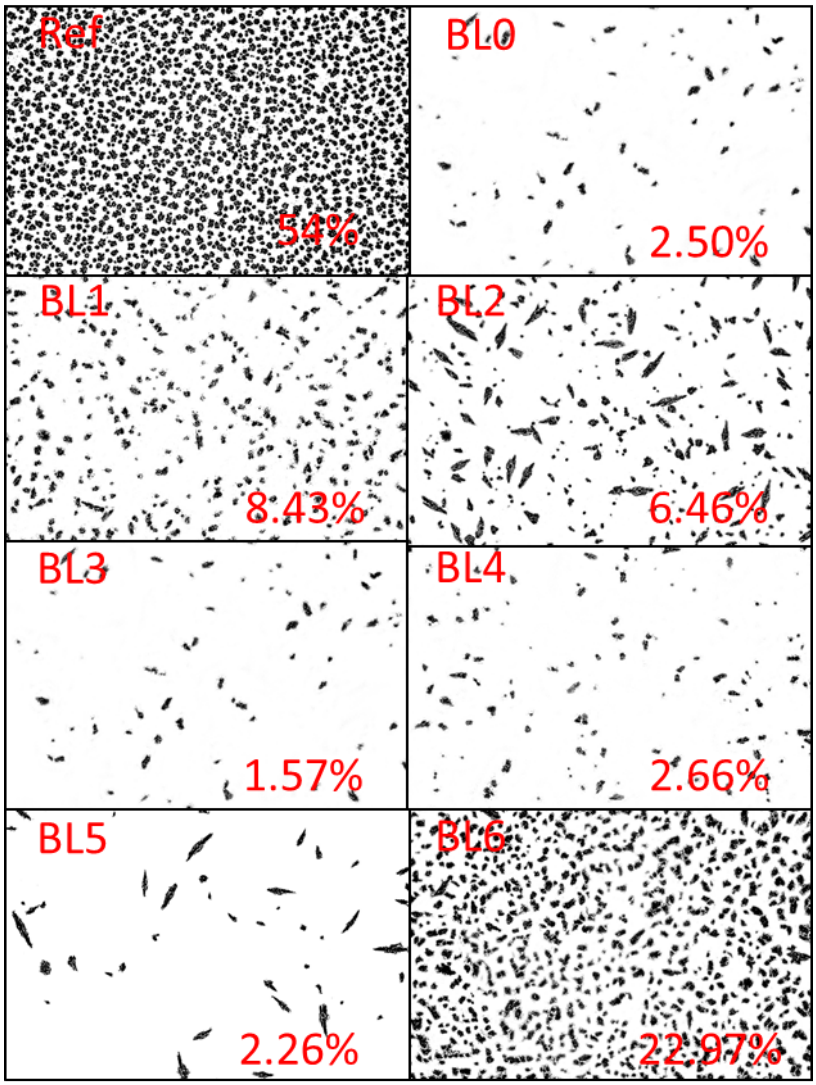

Fig. S5. Black-white pictures of P3HT:$PC_{61}BM$ blend films with different porphyrins after processing OM images shown in Figure 3.

As shown in **Figure S5,** those OM images in Figure 3 were converted into black-and-white photographs though Photoshop software**:** the $PC_{61}BM$ aggregates correspond the black regions while P3HT-rich domains without microscopic $PC_{61}BM$ aggregations correspond the white regions. Thus, the total area of black parts in the OM image captured at the same magnification was also used to calculate the degree of $PC_{61}BM$ aggregation.

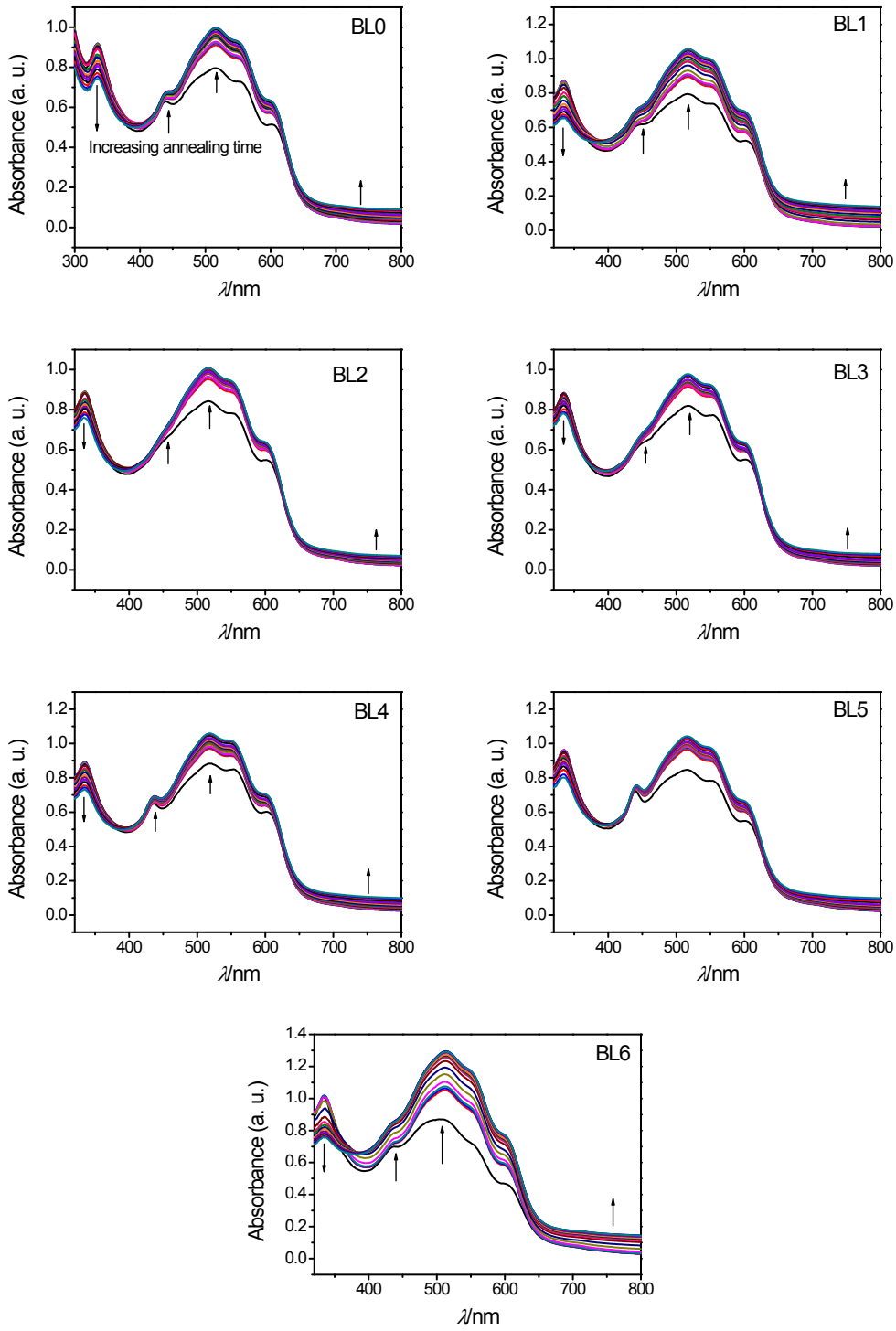

Fig. S6. UV-Vis absorption spectra of P3HT: $PC_{61}BM$ blend films with 3.78% of porphyrins during thermal annealing at 130 °C from 0 to 450 min.

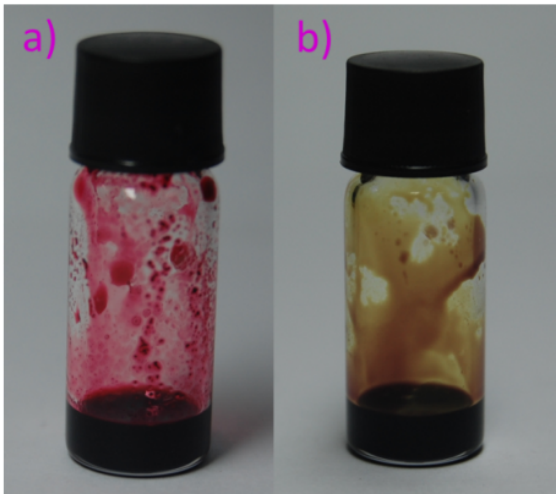

Fig. S7. Photographs of porphyrin solutions (a) BL4 solution standing for 2 days and (b) BL3 solution for half a year.

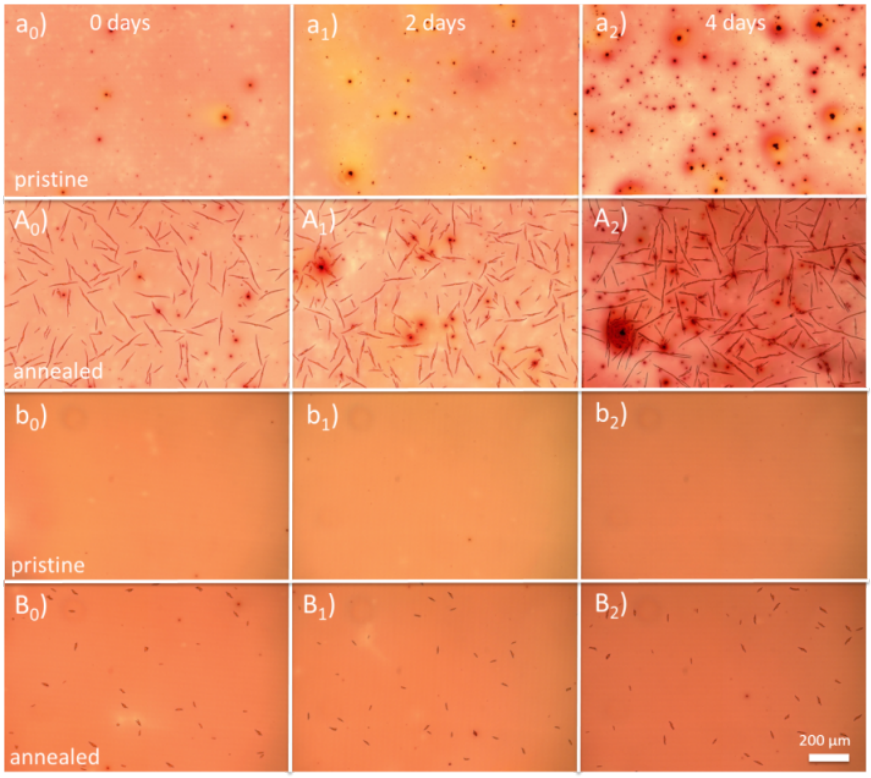

Fig. S8. OM images of P3HT: $PC_{61}BM$ blend films with 7.56% BL4 (a/A) and BL3 (b/B). The films spin-casted from the blend solution standing for 0, 2, and 4 days before (a_0-a_2, b_0-b_2) and after (A_0-A_2, B_0-B_2) 24 h annealing at 130 ^oC.

Table S3. Decaying of porphyrin solutions in ODCB after illumination calculated by peak absorption.

	BL0	BL1	BL2	BL3	BL4	BL5	BL6
λ/nm	422	428	434	431	420	424	418
A_p	1.24	0.96	1.01	1.06	0.99	1.10	1.11
A_i	0.67	0.36	0.87	1.05	0.85	0.11	0.93
A_d	45.97%	62.50%	13.87%	0.95%	14.15%	90.20%	16.22%

Note: A_p is the absorbance before illumination, and A_i is the absorbance after illumination. A_d is the percentage of degrading parts, defined as $1-A_i/ A_p$.

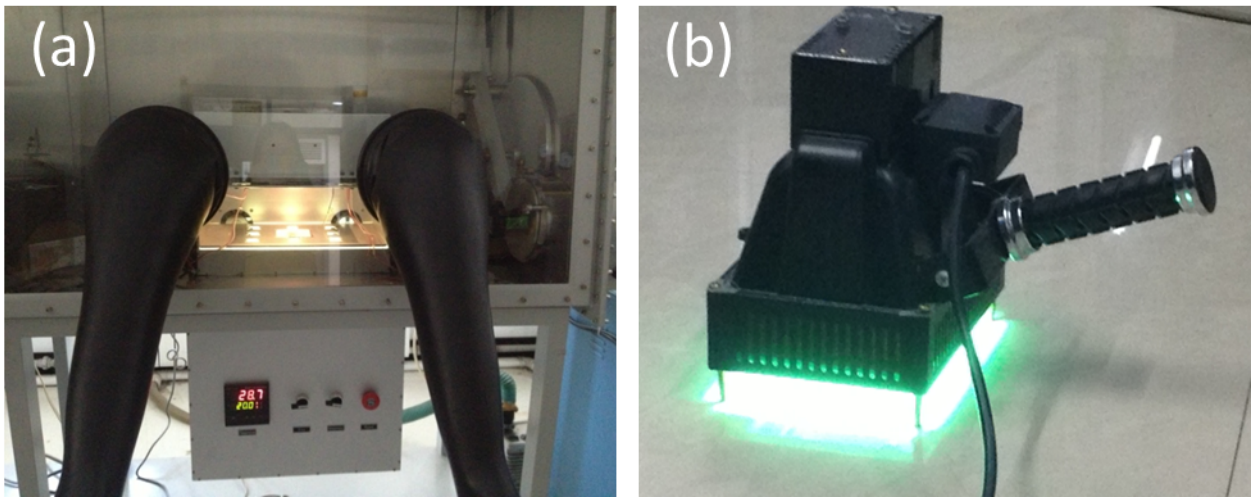

Fig. S9 The instruments for photo-degradation in (a) N_2 glove box and (b) atmosphere.

.

Table S4. Photovolatic parameters of devices based on P3HT:$PC_{61}BM$: 3.78% porphyrins blend films after isothermal annealing at 130 °C. All the active layer thicknesses were around 170 nm.

Sample device	Annealing time (h)	*Voc* (V)	*Jsc* (mA cm^{-2})	*FF* (%)	$PCE_{average}$ (%)	PCE_{best} (%)	η (%)
Ref	Pristine	0.54	-8.83	67.01	3.20	3.25	100
	3	0.56	-3.10	52.40	0.91	1.01	28.4
BL0	Pristine	0.54	-8.90	57.50	2.76	2.79	100
	3	0.54	-8.30	56.10	2.51	2.62	90.9
	12	0.54	-4.78	56.57	1.46	1.58	52.9
BL1	Pristine	0.54	-8.76	60.81	2.88	2.90	100
	3	0.54	-7.52	62.02	2.52	2.61	87.5
	12	0.54	-3.10	51.11	0.86	0.98	29.7
BL2	Pristine	0.54	-8.85	63.71	3.05	3.07	100
	3	0.54	-8.20	64.50	2.86	2.93	93.8
	12	0.54	-2.79	53.30	0.80	0.91	26.4
BL3	Pristine	0.56	-8.50	67.77	3.22	3.25	100
	3	0.54	-8.86	68.40	3.27	3.31	101.5
	12	0.54	-6.49	64.22	2.25	2.32	69.8
BL4	Pristine	0.54	-8.99	68.90	3.34	3.37	100
	3	0.54	-8.83	68.40	3.26	3.27	97.6
	12	0.56	-6.73	60.47	2.28	2.53	68.3
BL5	Pristine	0.54	-8.81	68.40	3.25	3.29	100
	3	0.56	-8.23	65.30	3.01	3.10	92.6
	12	0.54	-6.66	63.79	2.29	2.35	70.5
BL6	Pristine	0.54	-8.90	63.40	3.05	3.10	100
	3	0.58	-5.56	57.30	1.85	1.93	60.6
	12	0.52	-1.36	49.99	0.35	0.51	11.5

Note:

The relative efficiency η, which is defined as the ratio of PCE_t to PCE_0, PCE_t and PCE_0 are the efficiencies of the devices with active layers isothermally annealed at 150 °C for *t* and in pristine, respectively. The average PCE is obtained from 8 independent devices.

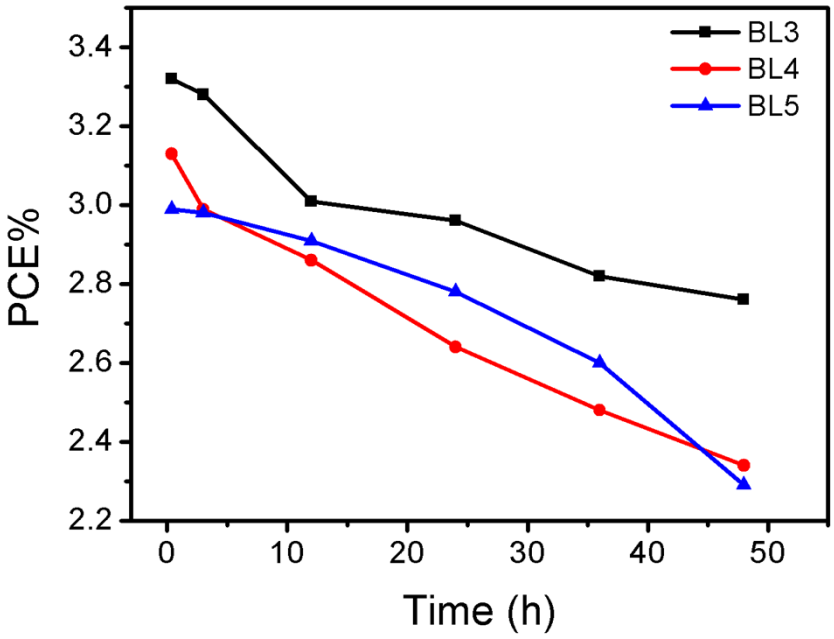

Fig. S10. Efficiency vs annealing time for P3HT:$PC_{61}BM$ devices loaded with 7.56% BL3, BL4 and BL5, respectively.

Table S5 Photovolatic parameters of devices based on P3HT:$PC_{61}BM$: 7.56% porphyrins blend films after isothermal annealing at 130 °C for different time. All the active layer thicknesses were around 170 nm.

Sample device	Annealing Time (h)	V_{oc} (V)	J_{sc} (mA cm^{-2})	*FF* (%)	$PCE_{average}$ (%)	PCE_{best} (%)	η (%)
BL3	Pristine	0.54	-9.01	68.27	3.32	3.36	100
	3	0.54	-9.19	66.14	3.28	3.30	98.8
	6	0.54	-8.76	64.50	3.05	3.10	91.9
	12	0.54	-8.55	65.29	3.01	3.05	90.7
	24	0.52	-8.37	67.97	2.96	2.99	89.1
	36	0.52	-7.97	67.95	2.82	2.94	84.9
	48	0.54	-7.86	65.00	2.76	2.82	83.1
BL4	Pristine	0.54	-8.58	65.14	3.13	3.16	100
	3	0.54	-8.99	61.04	2.96	3.01	94.8
	6	0.52	-8.89	61.42	2.84	2.90	91.0
	12	0.54	-8.88	59.58	2.86	2.88	91.6
	24	0.54	-8.61	56.85	2.64	2.71	84.6
	36	0.54	-7.68	59.95	2.48	2.52	79.5
	48	0.54	-7.28	59.57	2.34	2.41	75
BL5	Pristine	0.54	-8.49	65.29	2.99	3.02	100
	3	0.56	-8.17	65.16	2.98	3.02	99.6
	6	0.54	-8.58	62.65	2.90	2.96	96.9
	12	0.54	-8.44	63.78	2.91	2.95	97.3
	24	0.54	-8.16	63.04	2.78	2.82	92.9
	36	0.54	-7.77	62.07	2.61	2.73	87.3
	48	0.54	-6.46	63.43	2.29	2.46	76.6

Table S6 Photovolatic parameters of devices based on P3HT:$PC_{61}BM$ blends with and without 3.78% BL3 before and after isothermal annealing at 60 °C for one month. All the active layer thicknesses were around 170 nm.

Sample device	Annealing	V_{oc} (V)	J_{sc} (mA cm^{-2})	*FF* (%)	$PCE_{average}$ (%)	PCE_{best} (%)
Ref	before	0.54	-8.83	67.10	3.20	3.25
Ref	after	0.56	-7.59	67.30	2.86	2.88
BL3	before	0.56	-8.50	67.77	3.22	3.29
BL3	after	0.56	-8.45	68.07	3.22	3.27

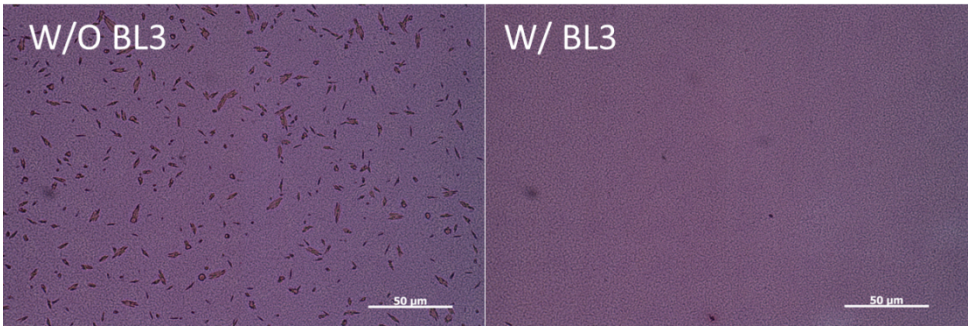

Fig. S11. OM images of P3HT: $PC_{61}BM$ blend films without and with 3.78% BL3 after annealing at 60 °C for one month.

Table S7 Photovolatic parameters of devices based on P3HT:$PC_{71}BM$ blends with and without 3.78% porphyrins after isothermal annealing at 150 °C for different time. All the active layer thicknesses were around 170 nm.

Sample device	Annealing time (h)	V_{oc} (V)	J_{sc} (mA cm^{-2})	*FF* (%)	$PCE_{average}$ (%)	PCE_{best} (%)	η (%)
W/O	Pristine	0.56	-9.29	68.60	3.57	3.60	100
	1	0.56	-9.24	67.98	3.52	3.56	98.6
	2	0.58	-8.14	65.35	3.09	3.16	86.5
	3	0.58	-5.95	59.74	2.06	2.18	57.7
	3.5	0.60	-5.09	55.75	1.70	1.78	47.6
	4.5	0.60	-4.32	54.20	1.40	1.51	39.2
	6.3	0.58	-4.32	55.11	1.38	1.43	38.6
	8.5	0.58	-3.21	51.76	0.96	1.02	26.9
	12	0.60	-2.94	49.94	0.88	0.98	24.6
W/	Pristine	0.56	-9.12	68.87	3.52	3.59	100
	1	0.56	-9.53	67.34	3.59	3.62	101.9
	3	0.56	-9.52	66.12	3.52	3.58	100
	6.3	0.56	-9.36	66.27	3.47	3.52	98.6
	12	0.56	-9.02	65.41	3.30	3.37	93.7
	20	0.56	-7.71	65.28	2.81	2.90	79.8
	24	0.56	-7.20	64.09	2.58	2.62	73.3
	32	0.56	-6.25	63.14	2.21	2.31	62.8

Reference

(1) Grimme, S., *J.Comput.Chem.* 2006, **27**, 1787-1799.

(2) Adamo, C.; Barone, V., *J .Chem. Phys* 1999, **110**, 6158-6170.

(3) Grimme, S., *WIREs Comput. Mol. Sci.* 2011, **1**, 211-228.

(4) Moreira, L.; Calbo, J.; Illescas, B. M.; Aragó, J.; Nierengarten, I.; Delavaux-Nicot, B.; Ortí, E.; Martín, N.; Nierengarten, J.-F., *Angew. Chem. Int. Ed.* 2015, **54**, 1255-1260.

(5) Dunning, T. H., Gaussian basis sets for use in correlated molecular calculations. I. *J. Chem. Phys.* 1989, **90**, 1007-1023.

(6) Grimme, S.; Ehrlich, S.; Goerigk, L., *J. Comput. Chem.* 2011, **32**, 1456-1465.

(7) M. J. Frisch, G. W. Trucks, H. B. Schlegel, G. E. Scuseria, M. A. Robb, J. R. Cheeseman, G. Scalmani, V. Barone, B. Mennucci, G. A. Petersson, H. Nakatsuji, M. Caricato, X. Li, H. P. Hratchian, A. F. Izmaylov, J. Bloino, G. Zheng, J. L. Sonnenberg, M. Hada, M. Ehara, K. Toyota, R. Fukuda, J. Hasegawa, M. Ishida, T. Nakajima, Y. Honda, O. Kitao, H. Nakai, T. Vreven, J. A. Montgomery, Jr., J. E. Peralta, F. Ogliaro, M. Bearpark, J. J. Heyd, E. Brothers, K. N. Kudin, V. N. Staroverov, R. Kobayashi, J. Normand, K. Raghavachari, A. Rendell, J. C. Burant, S. S. Iyengar, J. Tomasi, M. Cossi, N. Rega, J. M. Millam, M. Klene, J. E. Knox, J. B. Cross, V. Bakken, C. Adamo, J. Jaramillo, R. Gomperts, R. E. Stratmann, O. Yazyev, A. J. Austin, R. Cammi, C. Pomelli, J. W. Ochterski, R. L. Martin, K. Morokuma, V. G. Zakrzewski, G. A. Voth, P. Salvador, J. J. Dannenberg, S. Dapprich, A. D. Daniels, Ö. Farkas, J. B. Foresman, J. V. Ortiz, J. Cioslowski, and D. J. Fox, *Gaussian 09, Revision D.01*, Gaussian, Inc., Wallingford CT, 2009.